Geophysical Research Letters

RESEARCH LETTER
10.1029/2023GL104194

Diurnal Variability of the Upper Ocean Simulated by a Climate Model

J. E. Jack Reeves Eyre[1,2], Jieshun Zhu[2], Arun Kumar[2], and Wanqiu Wang[2]

[1]ERT Inc., Laurel, MD, USA, [2]Climate Prediction Center, NOAA/NWS/NCEP, College Park, MD, USA

Key Points:

- A 1-m vertical resolution ocean model accurately simulates global patterns of sea surface temperature mean diurnal cycle
- The model gives new insights into modes of subsurface ocean temperature and current diurnal variation
- Global maps of current diurnal cycle extend understanding past that from relatively sparse observations

Supporting Information:

Supporting Information may be found in the online version of this article.

Correspondence to:

J. E. J. Reeves Eyre,
jack.reeveseyre@gmail.com

Citation:

Reeves Eyre, J. E. J., Zhu, J., Kumar, A., & Wang, W. (2024). Diurnal variability of the upper ocean simulated by a climate model. *Geophysical Research Letters*, *51*, e2023GL104194. https://doi.org/10.1029/2023GL104194

Received 25 APR 2023
Accepted 30 OCT 2023

Author Contributions:

Conceptualization: J. E. Jack Reeves Eyre, Jieshun Zhu, Arun Kumar
Data curation: J. E. Jack Reeves Eyre, Jieshun Zhu
Formal analysis: J. E. Jack Reeves Eyre
Funding acquisition: Jieshun Zhu, Arun Kumar
Investigation: J. E. Jack Reeves Eyre
Methodology: J. E. Jack Reeves Eyre, Jieshun Zhu, Arun Kumar
Project Administration: Jieshun Zhu, Arun Kumar
Resources: Jieshun Zhu, Wanqiu Wang

Abstract We use a version of the NOAA Climate Forecast System with enhanced (up to 1-m) ocean model vertical resolution to investigate the mean diurnal cycles of upper ocean temperature and currents. The model sea surface temperature diurnal cycle agrees well with a global observational analysis. The simulated time-depth profiles of temperature and current also match closely observations from densely instrumented moorings in the tropical Pacific. Our analyses provide new insights into subsurface ocean diurnal cycles. Significant temperature diurnal range occurs, with seasonal modulation, at depths greater than 10 m across broad areas of the subtropical and midlatitude oceans. Significant current diurnal cycles are evident below 30 m across parts of the tropics, including in areas where deep-cycle turbulence has been observed.

Plain Language Summary We used computer model simulations of Earth's atmosphere and ocean to understand how ocean temperatures and currents vary by time of day. The model has 12 levels in the top 20 m of the ocean—greater than normal for this kind of simulation. This allows realistic simulated diurnal variations of sea surface temperature (compared to global observations), and realistic changes in temperature and current at and below the surface (compared to mooring observations). These results give us confidence in the global simulations of currents, which provide new insights into diurnal variations of surface ocean velocity and turbulence below the surface.

1. Introduction

The diurnal cycle of sea surface temperature (SST), while small compared to diurnal variations of land surface temperature, still has significant effects on the overlying atmosphere and the dynamics and thermodynamics of the near-surface ocean. Modeling the upper ocean diurnal variability is made difficult by the limited depth ($\lesssim$5 m) of diurnal warming compared to typical layer thickness ($\gtrsim$10 m) in the global ocean models used for weather and climate prediction applications. Model parameterizations (e.g., Large & Caron, 2015; Zeng & Beljaars, 2005) have been developed to simulate the diurnal cycle at the surface, with the aim of capturing the diurnal cycle of surface fluxes and their atmospheric response in general circulation models (GCMs). However, a dynamic ocean model with high vertical resolution is needed for simulation of the full spatiotemporal structure of oceanic diurnal variations. The aim of this paper is to evaluate one such model—a version of the NOAA Climate Forecast System (CFS) with 1-m vertical resolution in the upper ocean.

The diurnal cycle in the upper ocean is forced by the diurnal variation of solar radiation. During daytime, solar radiation is absorbed by the ocean, with transmission decreasing exponentially with depth. Surface-concentrated warming creates a density gradient, and stable stratification (Stable surface forcing like this can also occur due to rain.) Surface waves (due to wind and swell) can reduce the stable stratification, by causing vertical mixing. However, in conditions of light wind and strong solar radiation, vertical mixing can be limited enough to trap surface heat fluxes in a layer of only a few meters. This results in marked SST diurnal warming, leading to diurnal changes in lower atmospheric stability, surface fluxes (Clayson & Edson, 2019), cloud development and precipitation (Chen & Houze, 1997). Further, surface momentum fluxes can also be trapped in a shallow surface layer, causing diurnal jets in the current profile (Cronin & Kessler, 2009; Wenegrat & McPhaden, 2015; Masich et al., 2021, hereafter M21). In the right circumstances (a background state of marginal instability) these diurnal jets can produce shear instability and penetration of turbulence below the ocean mixed layer—so-called deep-cycle turbulence (Smyth & Moum, 2013). At nighttime, with the solar heat flux absent, the surface layer cools, inducing unstable stratification and vertical mixing, which usually return the upper ocean to a more uniform profile. For more detail, see Kawai and Wada (2007) and references therein.

Software: J. E. Jack Reeves Eyre
Supervision: Arun Kumar
Validation: J. E. Jack Reeves Eyre
Visualization: J. E. Jack Reeves Eyre
Writing – original draft: J. E. Jack Reeves Eyre
Writing – review & editing: Jieshun Zhu, Arun Kumar, Wanqiu Wang

Much of the physical understanding of the diurnal cycles over the ocean, particularly on deep-cycle turbulence, has come from a small number of highly instrumented near-equatorial moorings (Moum et al., 2022) and analysis of simulations in their vicinity (Cherian et al., 2021; Pei et al., 2020). Model simulations are thus required to understand wider spatiotemporal patterns, which depend on the complex interplay of latitude, winds, currents and clouds. Accurately simulating the diurnal warm layer and its effects places great demands on Earth system models. High vertical resolution (∼1-m vertical layer thickness) is needed to capture large gradients in the upper ocean (Bernie et al., 2005; Ge et al., 2017; Hsu et al., 2019). Due to these demands, some investigations of diurnal warming use 1-dimensional models (Brilouet et al., 2021; Giglio et al., 2017; Price et al., 1986). GCM simulations featuring such high resolution have shown changes in the simulation of mean SST (Guemas et al., 2013), tropical precipitation patterns and the Madden-Julian oscillation (Bernie et al., 2008; Seo et al., 2014; Shinoda et al., 2021; Zhu et al., 2020), as well as ocean circulation (Bernie et al., 2007).

The above studies notwithstanding, it is rare for global climate models to accurately and directly simulate the SST diurnal cycle. Past investigations show significant sensitivity of model results to the ocean warm layer diurnal cycle. These facts motivate the primary objectives of this study: to verify the NOAA Climate Forecast System version 2 (CFSv2) model's ability to simulate the diurnal cycles of SST and sub-surface temperature and current. If the diurnal variability is found to be realistic, then the consistent data provided by model simulations can be used to further advance our understanding of its various aspects, especially with respect to subsurface diurnal cycle.

2. Data and Methods

2.1. Model Simulation

The model simulation used in this study is the same as the CFSm501 experiment in Zhu et al. (2020). It uses the Climate Forecast System version 2 (CFSv2) model, modified with increased vertical resolution in the upper ocean and with the relaxed Arakawa-Schubert atmospheric convection scheme. Both modifications have been shown to improve simulations of intraseasonal climate signals (Zhang et al., 2019; Zhu et al., 2017). The ocean model has (starting from the surface) ten 1-m layers, two 5-m layers, then standard vertical resolution below depths of 20 m. Horizontal resolution of the ocean model is $0.5° \times 0.5°$ poleward of 30°, with meridional resolution increasing gradually to 0.25° between 10°S and 10°N. This free-running, coupled simulation is for 26 years. We analyze the final 4 years, which had hourly output from both ocean and atmosphere models. We analyze model temperature directly. For ocean current, we rotate coordinates to give the along-wind current and analyze the difference relative to a fixed reference depth of 60 m (as in Masich et al. (2021)). For simplicity, we refer to this quantity as ocean current.

2.2. Diurnal Cycle Metrics

We use hourly model output to calculate several metrics that characterize the diurnal cycles of temperature and current. We take the top model level (nominally at 0.5 m) to represent the surface values. We focus on monthly mean metrics on the model grid to effectively summarize the data but retain resolution of the seasonal cycle and spatial patterns. Monthly mean diurnal range can be characterized by either range of the monthly mean diurnal cycle or the monthly mean of the diurnal range (Section 2.2 in Wang & Zeng, 2014). We use the range of monthly mean diurnal cycle, because it is more closely linked to diurnal solar forcing (Wang & Zeng, 2014) and is methodologically closer to the observational data we use (Kennedy et al., 2007b). Phase of the diurnal cycle is characterized by the time of the maximum in the monthly mean diurnal cycle.

Depth variations of diurnal range are characterized by what we define as the threshold depth: the depth of the deepest model level with diurnal range greater than a fixed threshold (0.1 K for temperature; 2 cm s^{-1} for current). We found this to be more useful than either of the following options we explored. The depth at which diurnal range falls below a certain fraction of the surface value was too spatially uniform to be informative. The diurnal range at a fixed depth was too close to a "on-or-off" binary quantity. Depth variations of diurnal phase are characterized by the delay between the times of the surface diurnal maximum and the diurnal maximum at the threshold depth.

2.3. Observational Data

We use the Met Office Hadley Center's diurnal SST range data set (HadDTR; Kennedy et al., 2007a, 2007b) to assess the simulated diurnal cycle of SST. This is a gridded monthly climatology for the period 1990–2004,

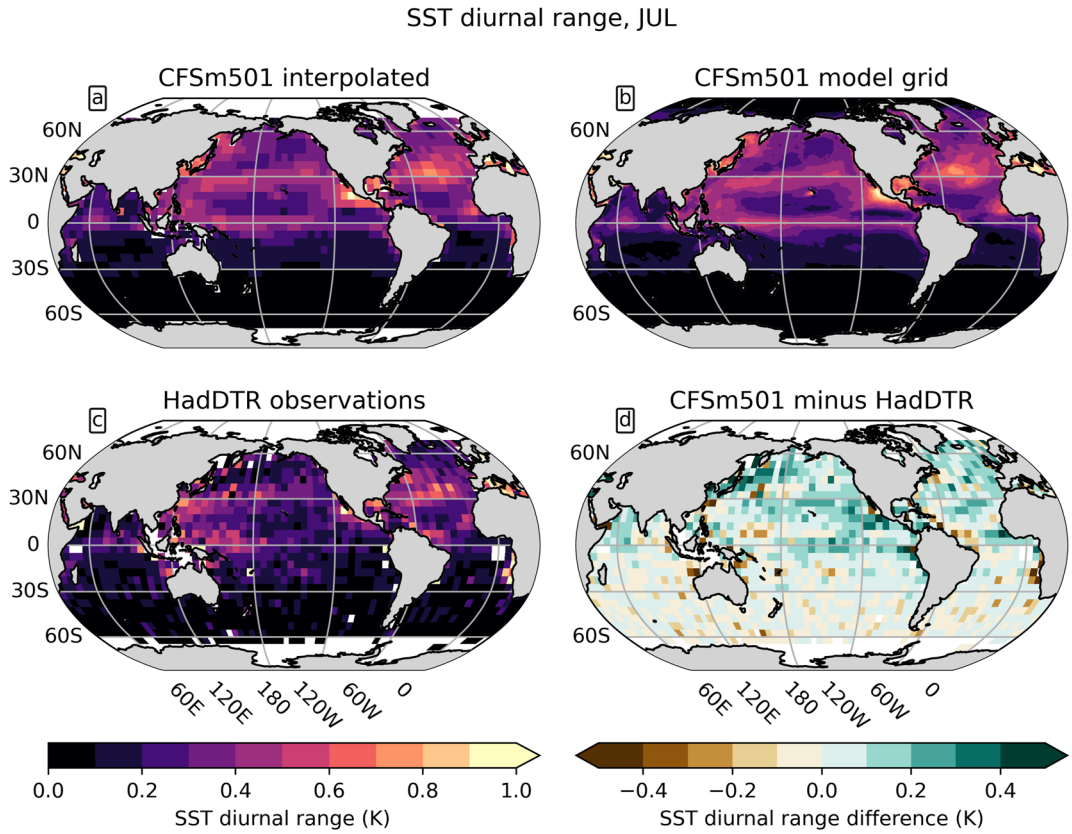

Figure 1. July mean sea surface temperature diurnal range from (a) CFSm501 interpolated to the HadDTR grid, (b) CFSm501 on the native model grid, (c) HadDTR observational data, and (d) the difference between CFSm501 and HadDTR. Note that CFSm501 data are nominally the 4-year average while HadDTR data are the 1990–2004 average.

constructed using hourly drifting buoy observations at around 25 cm depth. The data is on a 5° × 5° grid. We re-grid the model output to the 5° × 5° grid, using bilinear interpolation, for comparison purposes. Equivalent products for subsurface temperature are not available. Global observational current data sets (e.g., Rio et al., 2014) generally lack the temporal and vertical resolution to provide suitable verification for our model data and methods. Our results therefore likely provide some of the first global analysis of subsurface temperature and current diurnal cycles. We also verify the analysis with qualitative comparison against mooring-based studies.

3. Results

Figure 1 shows the July mean SST diurnal range from model (Figures 1a and 1b) and observations (Figure 1c). The key features in both are the small values south of 10°S and the large values on the equator and under the northern hemisphere subtropical highs. Maxima occur in the Mediterranean and off Mexico's Pacific coast. The spatial pattern in the simulation is similar to the observations. The noise apparent in the HadDTR map and the difference map (Figures 1c and 1d) suggests the HadDTR data might have considerable sampling uncertainties. The difference map (Figure 1d), however, also shows some systematic features. For example, the model diurnal range is too large over much of the eastern parts of the Pacific and Atlantic, as well as the Kuroshio current region. These systematic differences have several potential causes. Perhaps the most obvious is model bias, including clouds (Brunke et al., 2019) and radiation (e.g., Ge et al., 2017), and surface winds (Pradhan et al., 2022). Another potential cause is sampling error due to mismatch of time periods in observational and model data sets.

Results for January (Supporting Information S1, Figure S1) show similar features, with large values on the equator and in the southern hemisphere subtropical highs. However, the noise in the observational data appears to be larger in this season. Additionally, the model positive bias is more uniform than the more regionally concentrated biases in the northern hemisphere in July. From the results in Figure 1 and Figure S1 in Supporting

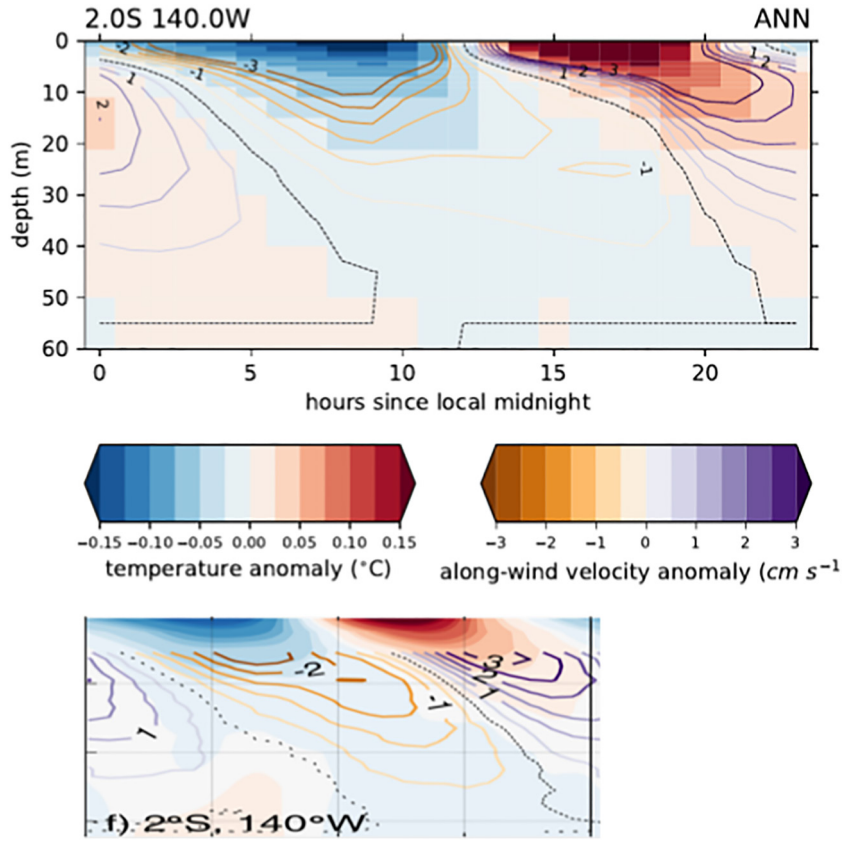

Figure 2. Annual mean ("ANN") anomalies, relative to the respective annual mean daily mean profiles, of temperature (color shading) and along-wind current (contours) at 2°S, 140°W. Along-wind current is calculated as the component in the direction of the annual mean daily mean wind, relative to that at 60 m depth. (top) Plotted from CFSm501 simulation. (bottom) Image taken from Figure 4 of Masich et al. (2021), showing observational data from the Tropical Atmosphere Ocean array mooring. The axis limits in the bottom panel are the same as in the top.

Information S1, CFSm501 seems to simulate reasonably well the SST monthly mean diurnal cycle, its spatial patterns and seasonal variability. We next turn to the other aspects of the upper ocean diurnal cycle.

Figure 2 shows model data from a single grid point in the eastern tropical Pacific. The presentation is based on M21 (their Figure 4), and the model results closely resemble their mooring observations. The main feature is the downward propagation, over the day, of the temperature and current diurnal cycles. The daytime warming and along-wind acceleration is somewhat sharper than the nighttime cooling and deceleration. This day-night asymmetry may reflect the different stabilizing and de-stabilizing effects that daytime heating and nighttime cooling have. The current data in M21 are only shown below 10 m depth, due to limitations of the upward looking acoustic doppler current profiler. Model output does not suffer from this issue, but using the same contours as M21 does not reveal much detail in the upper 10 m. We will see below that the surface current diurnal cycle can considerably exceed the 6 cm s-1 range shown in Figure 2. Model analysis (not shown) at the other sites analyzed in M21 reveals similar downward propagation in the eastern Pacific. Conversely, in the western Pacific, warming and diurnal current variation are limited to the upper 10 m of the ocean and there is little downward propagation. M21 shows the same east-west contrast in observations, which the authors attribute to strong background shear and marginal instability being present in the eastern and central Pacific but absent in the west.

Figures 1 and 2 demonstrate the realism of the model simulations and lend credibility to the other diurnal cycle metrics, shown in Figures 3 and 4, that cannot be compared with current observational coverage. Figures 3a and 3e reiterate the seasonal differences in SST diurnal range, with larger values in the summer hemisphere. The seasonal variations are most obvious in the subtropics and midlatitudes, presumably related to weaker solar radiation and more frequent high winds in winter. Figures 3b and 3f show that the phase is mostly dependent on

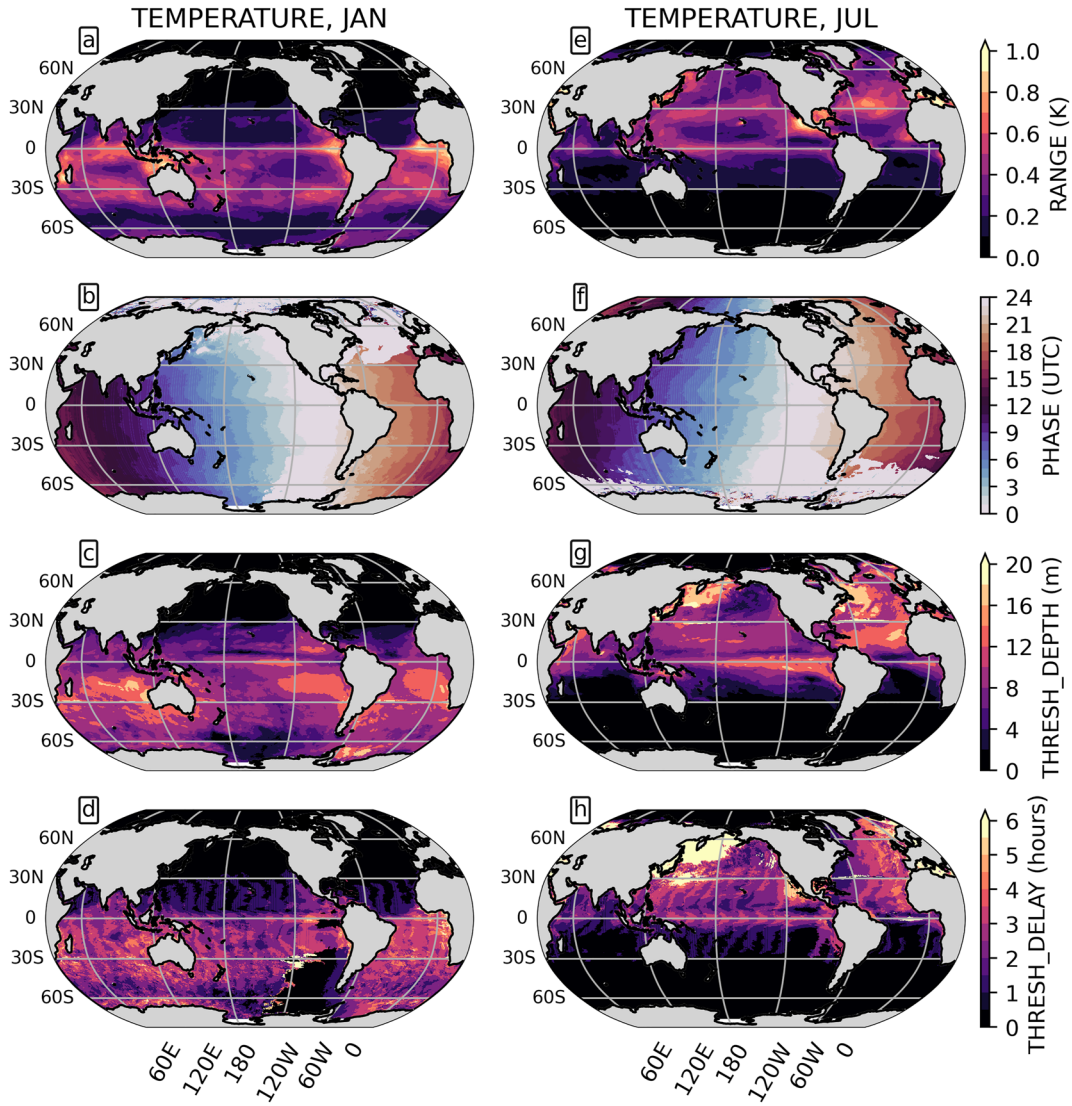

Figure 3. Ocean temperature diurnal cycle metrics for (left column) January and (right column) July. Metrics are: (a), (e) sea surface temperature diurnal range; (b), (f) time (UTC) of diurnal maximum; (c), (g) threshold depth, with threshold value of 0.1 K; (d), (h) phase delay at threshold depth.

longitude, with diurnal maxima occurring in the afternoons. Maxima occur slightly later in the summer hemisphere than the winter hemisphere.

To investigate the wider spatial variation of this downward propagation, we look at the threshold depth metric for temperature (Figures 3c and 3g). High values tend to be concentrated in the eastern ocean basins, but also close to western boundary currents. There are marked latitudinal variations too, for example, high values on the equator, low values at 5°N, and high values at 10°N. Spatial variations have a complex relationship with the SST diurnal range (Figures 3a and 3e). For example, the relationship is an inverse one across the tropical Pacific: high SST diurnal range with small threshold depth in the western Pacific, and low SST diurnal range and large threshold depth in the eastern Pacific. Conversely, the relationship is linear across the mid-latitude Pacific (e.g., 45°N). The complexity of these relationships may reflect the variety of controlling physical processes. Large scale factors—latitude and season—control the diurnal cycle of surface heating. But the effect of this heating on surface and subsurface temperature is strongly affected by winds and currents, which can vary on smaller spatiotemporal scales.

The tropical Pacific presents several regimes across relatively small spatial regions. In the western equatorial Pacific, light winds and relatively little current shear result in a strong SST diurnal cycle with minimal downward propagation. Further east on the equator, winds are slightly stronger and there is significant vertical shear

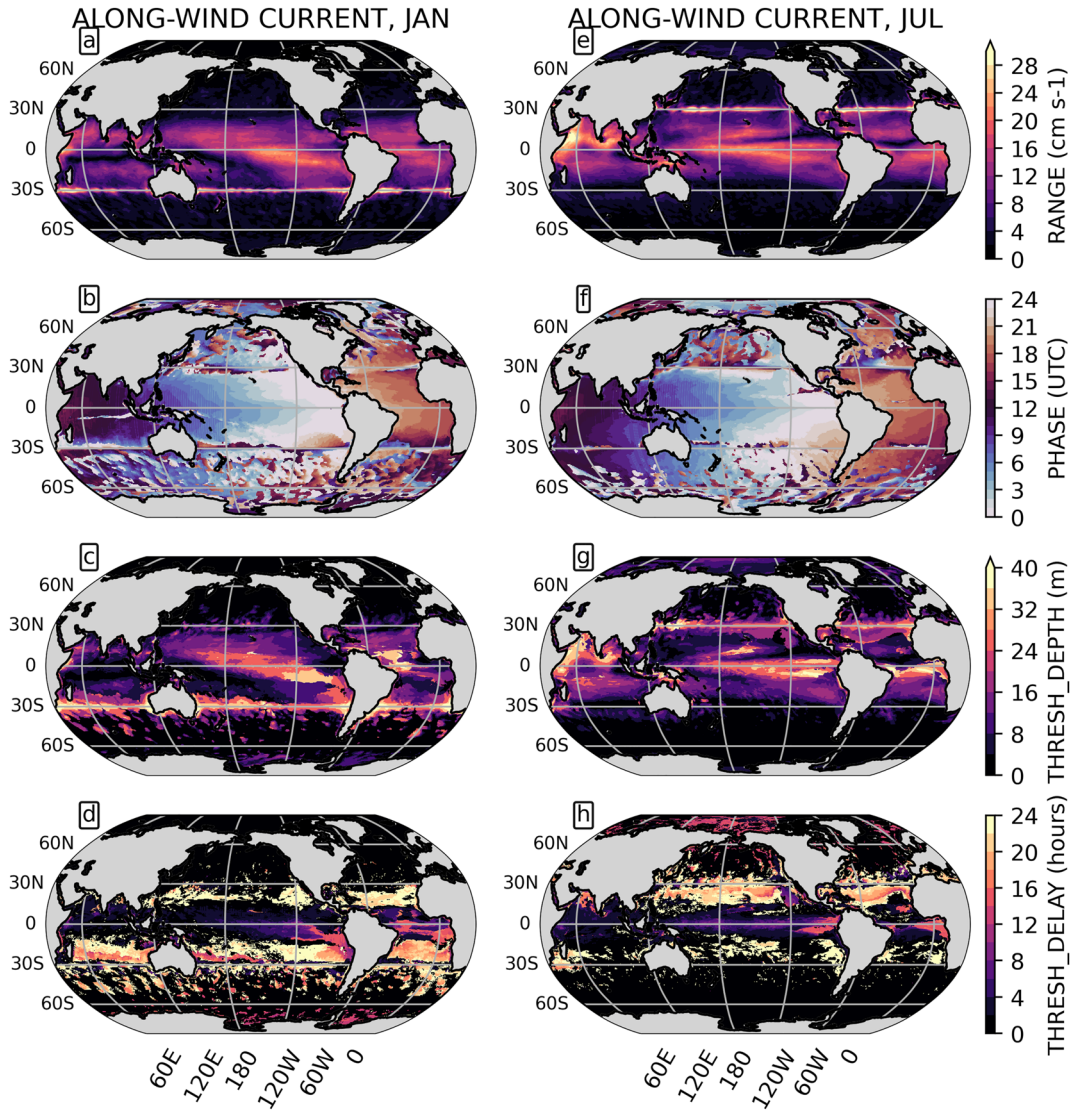

Figure 4. As Figure 3 but for along-wind current. Note that panels (c), (d), (g), and (h) use different color scales to Figure 3.

of the zonal current. This combination results in a large SST diurnal cycle, which propagates downwards during the course of the afternoon and evening (see large values around 120°W in both Figures 3c and 3d). Away from the equator (e.g., 15°N, 180°W), consistently strong trade winds limit the SST diurnal range, but also cause a relatively large threshold depth (indicating that surface warming is spread over a deeper layer; Figures 3c and 3g) and small phase delay at threshold depth (indicating surface-forced mixing, rather than the gradual descent of turbulence; Figures 3d and 3h).

For current diurnal cycles we see, as with temperature, large surface diurnal range values across much of the tropics (Figures 4a and 4e). However, there is one distinct feature not shared with the temperature results: the stripe of high diurnal range values at 30°S and 30°N. Although clear in the diurnal cycle metrics, the stripes do not appear in the monthly mean current (Figure S2 in Supporting Information S1) or even the diurnal range of an individual day (Figure S3 in Supporting Information S1). We considered a number of possible explanations for the stripes, and we believe them to be caused by inertial oscillations. At 30°, inertial oscillations have a period of exactly 1 day. It is therefore possible for them to have a consistent phase (e.g., maxima at midnight UTC) throughout a month, and therefore the oscillation is resolved by the monthly mean diurnal cycle. Only a few degrees latitude away from 30°, the period is different enough from 24 hr that the phase shifts through the course of the month (Figure S4 in Supporting Information S1). Averaging over long enough periods therefore results in cancellation

between different phases of inertial oscillation, except very close to 30° latitude (Figures S5–S7 in Supporting Information S1). One remaining puzzle in this explanation, however, is that for inertial oscillations to consistently appear in the monthly average at 30°, they must have consistent phase, which suggests they must experience forcing with a fixed, diurnal phase. One possibility is that winds associated with atmospheric tides can fulfill this role (Stockwell et al., 2004), though Figure S4 in Supporting Information S1 does not provide evidence of this, at least visually. In coastal regions, the diurnal cycle of land- and sea-breezes can also provide the necessary forcing (Simpson et al., 2002).

Aside from the stripes at 30°S and 30°N, the diurnal cycle metrics seem plausible and realistic. In the tropics, there are quite large areas with 20 cm s^{-1} surface diurnal range, and local maxima in the central tropical Pacific, equatorial Atlantic and western Indian ocean. The current diurnal phase (Figures 4b and 4f) has more complicated patterns than temperature, with a series of bands across different latitudes.

Compared with the surface versus depth relationship for temperature, the surface versus depth relationship for current (Figures 4c and 4g) seems to be quite linear (The relationship is clear in Figures S8 and S9 in Supporting Information S1). This may be because the regions with significant surface diurnal cycles of current (mostly between 20°S and 20°N) are more limited than for SST. Therefore, the range of atmospheric, oceanic and geographic conditions affecting the diurnal variations is smaller. The main features of the along-wind current threshold depth are large values in the central and eastern tropical Pacific, the tropical Atlantic, and the Arabian sea. These coincide with the large diurnal range at the surface. Interestingly, they are all areas of cool SST (relative to surroundings) and upwelling. Even the seasonality of the threshold depth follows this pattern. Large values in the Arabian Sea occur in July but not January, related to seasonal upwelling and cooling caused by the southwest monsoon. Large values in the Atlantic occur mainly in the west, including north of the equator, in January—a time when the warmest water is found further east. But in July, when warm water stretches across the Atlantic at about 5°N, the large threshold depth values occur south of the equator and in the east. Phase delays (Figures 4d and 4h) of around 12 hr occur across much of the area with large threshold depth values, suggestive of a true downward propagation signal (as in Figure 2), not just vigorous wind-driven mixing. In some regions, like the equatorial Pacific and Atlantic, this indicates the occurrence of deep-cycle turbulence. However, in regions with greater thermocline depths, the gradual downward propagation of current acceleration is not true deep-cycle turbulence but may instead be part of night-time erosion of the diurnal warm layer.

4. Conclusions

In this study we have looked at the upper ocean mean diurnal cycles of temperature and current in a modified version of CFSv2. Comparison with a global observational data set for SST diurnal range shows the simulations are accurate and realistic in terms of magnitude and spatial patterns. Examination of model profiles at locations used in M21 reveals the sub-surface temperature and current diurnal cycles are also realistic. The accuracy and realism revealed in these observational verifications suggests that the ocean model's high vertical resolution has the desired effect. This means that we can place reasonable trust even in the aspects of simulated upper ocean diurnal cycle that do not have global verification data sets.

Subsurface temperature diurnal cycles reach below ∼10 m depth across quite broad stretches of the global oceans. This includes equatorial regions, as in mooring data (including M21). But also, eastern subtropical oceans and western boundary currents have relatively deep temperature diurnal cycles, at least in summer. The diurnal range of surface currents commonly exceed 20 cm s^{-1} in tropical oceans. This is significantly more than the diurnal range at 10 m seen in observations in M21. These simulated surface currents are hard to verify with acoustic doppler current profilers and standard in situ current measurements. However, some observational results do support this significant vertical shear in the upper 10 m of the oceans (Laxague et al., 2018). Our results also show significant subsurface current diurnal cycles, along with time delays that point to gradual downward propagation of turbulence. It is important to note here that the vertical resolution of our model reverts to the standard 10 m below 20 m depth, so fine scale vertical gradients away from the surface cannot be simulated. Nonetheless, configurations of ocean vertical resolution similar to ours have been used successfully to analyze deep-cycle turbulence (Pei et al., 2020; Shinoda et al., 2021). Building on the accuracy at mooring locations, our results suggest that downward propagating turbulence (including deep-cycle turbulence) is quite widespread in the tropical oceans.

Our work has focused on the upper ocean mean diurnal cycle. We have shown that 1-m vertical resolution results in realistic temperature and along-wind current variations at diurnal timescales. Future work could extend this to salinity variations and barrier layers, as well as cross-wind current and rotation of current with depth. In addition, a similar analysis of surface fluxes and the near-surface atmosphere could be illuminating. There is ample evidence that realistic SST diurnal cycles can improve simulations of mean SST, precipitation patterns and the Madden Julian Oscillation. However, there is much left to learn about the physical processes that cause these improvements through changes in surface fluxes and the near-surface atmosphere. Future investigations of these topics would be informative and valuable.

Data Availability Statement

The software and data used to create the plots are freely and publicly available (Reeves Eyre, 2023a, 2023b). Raw simulation output data is available through Zhu et al. (2020). The HadDTR data (Kennedy et al., 2007a) are freely and publicly available online.

Acknowledgments
We are grateful to Hui Wang and Zeng-Zhen Hui for valuable suggestions on the manuscript. We thank Meghan Cronin for discussions that led to the explanation of current diurnal cycle stripes at 30° latitude. We thank the editor and two anonymous reviewers for their constructive comments that greatly improved the manuscript. This work was supported by the NOAA Global Ocean Monitoring and Observing program and NOAA Oceanic and Atmospheric Research.

References

Bernie, D. J., Guilyardi, E., Madec, G., Slingo, J. M., & Woolnough, S. J. (2007). Impact of resolving the diurnal cycle in an ocean–atmosphere GCM. Part 1: A diurnally forced OGCM. *Climate Dynamics*, *29*(6), 575–590. https://doi.org/10.1007/s00382-007-0249-6

Bernie, D. J., Guilyardi, E., Madec, G., Slingo, J. M., Woolnough, S. J., & Cole, J. (2008). Impact of resolving the diurnal cycle in an ocean–atmosphere GCM. Part 2: A diurnally coupled CGCM. *Climate Dynamics*, *31*(7), 909–925. https://doi.org/10.1007/s00382-008-0429-z

Bernie, D. J., Woolnough, S. J., Slingo, J. M., & Guilyardi, E. (2005). Modeling diurnal and intraseasonal variability of the ocean mixed layer. *Journal of Climate*, *18*(8), 1190–1202. https://doi.org/10.1175/JCLI3319.1

Brilouet, P.-E., Redelsperger, J.-L., Bouin, M.-N., Couvreux, F., & Lebeaupin Brossier, C. (2021). A case-study of the coupled ocean–atmosphere response to an oceanic diurnal warm layer. *Quarterly Journal of the Royal Meteorological Society*, *147*(736), 2008–2032. https://doi.org/10.1002/qj.4007

Brunke, M. A., Ma, P.-L., Reeves Eyre, J. E. J. R., Rasch, P. J., Sorooshian, A., & Zeng, X. (2019). Subtropical marine low stratiform cloud deck spatial errors in the E3SMv1 atmosphere model. *Geophysical Research Letters*, *46*(21), 12598–12607. https://doi.org/10.1029/2019GL084747

Chen, S. S., & Houze, R. A., Jr. (1997). Diurnal variation and life-cycle of deep convective systems over the tropical Pacific warm pool. *Quarterly Journal of the Royal Meteorological Society*, *123*(538), 357–388. https://doi.org/10.1002/qj.49712353806

Cherian, D. A., Whitt, D. B., Holmes, R. M., Lien, R.-C., Bachman, S. D., & Large, W. G. (2021). Off-equatorial deep-cycle turbulence forced by tropical instability waves in the equatorial Pacific. *Journal of Physical Oceanography*, *51*(5), 1575–1593. https://doi.org/10.1175/JPO-D-20-0229.1

Clayson, C. A., & Edson, J. B. (2019). Diurnal surface flux variability over Western boundary currents. *Geophysical Research Letters*, *46*(15), 9174–9182. https://doi.org/10.1029/2019GL082826

Cronin, M. F., & Kessler, W. S. (2009). Near-surface shear flow in the tropical Pacific cold Tongue front. *Journal of Physical Oceanography*, *39*(5), 1200–1215. https://doi.org/10.1175/2008JPO4064.1

Ge, X., Wang, W., Kumar, A., & Zhang, Y. (2017). Importance of the vertical resolution in simulating SST diurnal and intraseasonal variability in an oceanic general circulation model. *Journal of Climate*, *30*(11), 3963–3978. https://doi.org/10.1175/JCLI-D-16-0689.1

Giglio, D., Gille, S. T., Subramanian, A. C., & Nguyen, S. (2017). The role of wind gusts in upper ocean diurnal variability. *Journal of Geophysical Research: Oceans*, *122*(9), 7751–7764. https://doi.org/10.1002/2017JC012794

Guemas, V., Salas-Mélia, D., Kageyama, M., Giordani, H., & Voldoire, A. (2013). Impact of the ocean diurnal cycle on the North Atlantic mean sea surface temperatures in a regionally coupled model. *Dynamics of Atmospheres and Oceans*, *60*, 28–45. https://doi.org/10.1016/j.dynatmoce.2013.01.001

Hsu, J.-Y., Hendon, H., Feng, M., & Zhou, X. (2019). Magnitude and phase of diurnal SST variations in the ACCESS-S1 model during the suppressed phase of the MJOs. *Journal of Geophysical Research: Oceans*, *124*(12), 9553–9571. https://doi.org/10.1029/2019JC015458

Kawai, Y., & Wada, A. (2007). Diurnal sea surface temperature variation and its impact on the atmosphere and ocean: A review. *Journal of Oceanography*, *63*(5), 721–744. https://doi.org/10.1007/s10872-007-0063-0

Kennedy, J. J., Brohan, P., & Tett, S. F. (2007a). Haddtr: Hadley centre sea-surface temperature diurnal temperature range climatology [Dataset]. Met Office Hadley Center. Retrieved from https://www.metoffice.gov.uk/hadobs/haddtr/

Kennedy, J. J., Brohan, P., & Tett, S. F. B. (2007b). A global climatology of the diurnal variations in sea-surface temperature and implications for MSU temperature trends. *Geophysical Research Letters*, *34*(5), L05712. https://doi.org/10.1029/2006GL028920

Large, W. G., & Caron, J. M. (2015). Diurnal cycling of sea surface temperature, salinity, and current in the CESM coupled climate model. *Journal of Geophysical Research: Oceans*, *120*(5), 3711–3729. https://doi.org/10.1002/2014JC010691

Laxague, N. J. M., Özgökmen, T. M., Haus, B. K., Novelli, G., Shcherbina, A., Sutherland, P., et al. (2018). Observations of near-surface current shear help describe oceanic oil and plastic Transport. *Geophysical Research Letters*, *45*(1), 245–249. https://doi.org/10.1002/2017GL075891

Masich, J., Kessler, W. S., Cronin, M. F., & Grissom, K. R. (2021). Diurnal cycles of near-surface currents across the tropical Pacific. *Journal of Geophysical Research: Oceans*, *126*(4), e2020JC016982. https://doi.org/10.1029/2020JC016982

Moum, J. N., Hughes, K. G., Shroyer, E. L., Smyth, W. D., Cherian, D., Warner, S. J., et al. (2022). Deep cycle turbulence in Atlantic and Pacific cold tongues. *Geophysical Research Letters*, *49*(8), e2021GL097345. https://doi.org/10.1029/2021GL097345

Pei, S., Shinoda, T., Wang, W., & Lien, R.-C. (2020). Simulation of deep cycle turbulence by a global ocean general circulation model. *Geophysical Research Letters*, *47*(15), e2020GL088384. https://doi.org/10.1029/2020GL088384

Pradhan, M., Rao, S. A., Bhattacharya, A., & Balasubramanian, S. (2022). Improvements in diurnal cycle and its impact on seasonal mean by incorporating COARE flux algorithm in CFS. *Frontiers in Climate*, *3*. https://doi.org/10.3389/fclim.2021.792980

Price, J. F., Weller, R. A., & Pinkel, R. (1986). Diurnal cycling: Observations and models of the upper ocean response to diurnal heating, cooling, and wind mixing. *Journal of Geophysical Research*, *91*(C7), 8411–8427. https://doi.org/10.1029/JC091iC07p08411

Reeves Eyre, J. E. J. (2023a). cfs-analysis-gaea v0.1.2: Diurnal cycle—Revised submission to journal [Software]. Github. https://doi.org/10.5281/zenodo.7846095

Reeves Eyre, J. E. J. (2023b). Data accompanying "diurnal variability of the upper ocean simulated by a climate model" [Dataset]. Zenodo. https://doi.org/10.5281/zenodo.7846473

Rio, M.-H., Mulet, S., & Picot, N. (2014). Beyond GOCE for the ocean circulation estimate: Synergetic use of altimetry, gravimetry, and in situ data provides new insight into geostrophic and Ekman currents. *Geophysical Research Letters*, *41*(24), 8918–8925. https://doi.org/10.1002/2014GL061773

Seo, H., Subramanian, A. C., Miller, A. J., & Cavanaugh, N. R. (2014). Coupled impacts of the diurnal cycle of sea surface temperature on the Madden–Julian oscillation. *Journal of Climate*, *27*(22), 8422–8443. https://doi.org/10.1175/JCLI-D-14-00141.1

Shinoda, T., Pei, S., Wang, W., Fu, J. X., Lien, R.-C., Seo, H., & Soloviev, A. (2021). Climate process team: Improvement of ocean component of NOAA climate forecast system relevant to Madden-Julian oscillation simulations. *Journal of Advances in Modeling Earth Systems*, *13*(12), e2021MS002658. https://doi.org/10.1029/2021MS002658

Simpson, J. H., Hyder, P., Rippeth, T. P., & Lucas, I. M. (2002). Forced oscillations near the critical latitude for diurnal-inertial resonance. *Journal of Physical Oceanography*, *32*(1), 177–187. https://doi.org/10.1175/1520-0485(2002)032⟨0177:FONTCL⟩2.0.CO;2

Smyth, W. D., & Moum, J. N. (2013). Marginal instability and deep cycle turbulence in the eastern equatorial Pacific Ocean. *Geophysical Research Letters*, *40*(23), 6181–6185. https://doi.org/10.1002/2013GL058403

Stockwell, R. G., Large, W. G., & Milliff, R. F. (2004). Resonant inertial oscillations in moored buoy ocean surface winds. *Tellus*, *56*(5), 536–547. https://doi.org/10.1111/j.1600-0870.2004.00086.x

Wang, A., & Zeng, X. (2014). Range of monthly mean hourly land surface air temperature diurnal cycle over high northern latitudes. *Journal of Geophysical Research: Atmospheres*, *119*(10), 2014JD021602. https://doi.org/10.1002/2014JD021602

Wenegrat, J. O., & McPhaden, M. J. (2015). Dynamics of the surface layer diurnal cycle in the equatorial Atlantic Ocean (0°, 23°W). *Journal of Geophysical Research: Oceans*, *120*(1), 563–581. https://doi.org/10.1002/2014JC010504

Zeng, X., & Beljaars, A. (2005). A prognostic scheme of sea surface skin temperature for modeling and data assimilation. *Geophysical Research Letters*, *32*(14), L14605. https://doi.org/10.1029/2005GL023030

Zhang, Y., Hung, M.-P., Wang, W., & Kumar, A. (2019). Role of SST feedback in the prediction of the boreal summer monsoon intraseasonal oscillation. *Climate Dynamics*, *53*(7), 3861–3875. https://doi.org/10.1007/s00382-019-04753-w

Zhu, J., Kumar, A., & Wang, W. (2020). Intraseasonal surface salinity variability and the MJO in a climate model. *Geophysical Research Letters*, *47*(17), e2020GL088997. https://doi.org/10.1029/2020GL088997

Zhu, J., Wang, W., & Kumar, A. (2017). Simulations of MJO propagation across the maritime continent: Impacts of SST feedback. *Journal of Climate*, *30*(5), 1689–1704. https://doi.org/10.1175/JCLI-D-16-0367.1